Physica A 583 (2021) 126301

Contents lists available at ScienceDirect

Physica A

journal homepage: www.elsevier.com/locate/physa

Analysis of road capacity and pollutant emissions: Impacts of Connected and automated vehicle platoons on traffic flow

Ke Ma [a,d], Hao Wang [a,b,c,*], Tiancheng Ruan [a,b,c]

[a] Jiangsu Key Laboratory of Urban ITS, Southeast University, 2 Si pai lou, Nanjing, People's Republic of China
[b] Jiangsu Province Collaborative Innovation Center of Modern Urban Traffic Technologies, Southeast University, 2 Si pai lou, Nanjing, People's Republic of China
[c] School of Transportation, Southeast University, 2 Si pai lou, Nanjing, People's Republic of China
[d] Department of Civil and Environmental Engineering, University of South Florida, 4202 E Fowler Avenue, ENC 3300, Tampa, FL 33620

ARTICLE INFO

Article history:
Received 30 November 2020
Received in revised form 26 June 2021
Available online 4 August 2021

Keywords:
Connected and Automated Vehicle
Mixed traffic flow
Road capacity
ACC and CACC system
Traffic simulation
Pollutant emissions

ABSTRACT

Connected and Automated Vehicles (CAV) are currently not intelligent enough to deal with complex traffic conditions. CAVs traveling in platoons can reduce external interference and further improve road capacity. Therefore, a mixed traffic capacity gain formula was constructed, considering both communication interaction and size limitations of CAV platoons. CAVs are divided into three types in a mixed traffic environment in terms of different states and positions. A model was constructed to examine how several parameters affect capacity, and these capacity-improving parameters were used to indicate coefficients of headway gains. Additionally, an empirical formula for pollutant emissions with different headway gains is applied in the mixed traffic. A series of microsimulations are tested based on the improved Full Velocity Difference (FVD) model and CAV models which are established as discrete steps based on the above analyses. The simulation results are highly consistent with the theoretical analyses, demonstrating the universality of this model. Finally, it indicated that the overall optimal size of CAV platoons is between 5 and 10 when taking both the road capacity and pollutant emissions into consideration.

1. Introduction

With the development of the urbanization process, urban and highway traffic problems are increasing significantly. They are mainly manifested in severe traffic congestion, traffic accident rate, and environmental problem [1–4]. Among them, traffic congestion and pollutant emissions have attracted much attention from government departments, scholars, and engineers. However, suppose the driving behavior of the participants in traffic activities cannot be effectively improved. In that case, problems such as the improvement of traffic operation efficiency [5,6] and gas emissions [4,7] will not be fundamentally changed. The development of the Internet of vehicle technology and automated driving technology makes it possible to solve the above problems. Multi-vehicles collaborative lane-changing behavior [8], speed collaborative optimization [9,10], high-speed driving on-ramps [11,12], and intersections have also become new research hotspots due to the development of artificial intelligence and communication technology.

* Corresponding author at: School of Transportation, Southeast University, Nanjing, People's Republic of China.
E-mail addresses: kema@seu.edu.cn (K. Ma), haowang@seu.edu.cn (H. Wang), 230198696@seu.edu.cn (T. Ruan).

https://doi.org/10.1016/j.physa.2021.126301
0378-4371/

Fig. 1. CAV information flow topologies.

To realize the safe and efficient driving of Connected and Automated Vehicles (CAVs) on the road as soon as possible, scholars have conducted many simulation analyses on the running characteristics of CAVs under Vehicle to Vehicle (V2V) environment, including road capacity and pollutant emissions. Among them, the most typical applications of V2V communication are Adaptive Cruise Control (ACC) and Cooperative Adaptive Cruise Control (CACC) [13–16], which enable CAVs to automatically maintain a fixed time interval with the preceding vehicle. In both simulation experiments and field experiments, it is generally believed that continuous CAVs can maintain a smaller headway than traditional Manual Vehicles (MVs) to improve road capacity and reduce pollutant emissions. Therefore, continuous CAV platoons have become an important factor to improve highway capacity.

The forming of CAV platoons mainly depends on the V2V communication protocol and roadside infrastructure communication protocol [17–21]. Queued and continuous CAV platoons can transcend the inherent limitations of on-board sensors on a single-vehicle and ensure CAVs' safety and efficiency by timely acquiring surrounding information. These platoons can also improve the driving experience and traffic efficiency based on behavior decisions and travel control. Having analyzed CAV Market Penetration Rate (MPR) and CACC/ACC control system [22–25], this paper prospectively explores the impact of CAVs on capacity gain and pollutant emissions before the emergence of large-scale mixed traffic flows based on the statistical characteristics of mixed traffic and simulation models.

For a quite long time to come, the road will generally witness a mixed traffic flow that consists of both CAVs and MVs. In this paper, we focus on the traffic flow on the single lane, and vehicles are randomly and uniformly set on the road. So far, most of the work has used microsimulation [16,17] or limited theoretical analyses [21–25] to describe the characters of mixed traffic flow. However, these researches lack a comprehensive construction of theory and simulation. To bridge the gaps between the studies of CAV platoon size and traffic operations, this paper provides a general theoretical formula to illustrate how capability varies with CAV MPR.

In this paper, capacity refers to the maximum sustainable flow rate of a section given CAV MPR. This is an essential step in establishing benchmarks to fully understand the impact of micro-characteristics (such as platoons length and spacing), which are demonstrated with a single parameter, the critical headway of CAV. Thus, a clear relationship with the macroscopic capacity is established. We further developed a general formula, including CAV platoon size limitations and headway gains, to determine the distribution and capacity changes under a given CAVs communication capability, CAV MPR, and headway gains. Besides, based on the above analyses, this paper explored the influence of the mixed traffic flow on environmental emissions under different topology model conditions and CAV platoon size limitations.

2. Modes and communication

The communication module of the CAV system mainly relies on real-time and reliable wireless V2V and vehicle-to-infrastructure (V2I) technologies. The bandwidth of these two communication methods is insufficient as the number of CAVs increases within the coverage area. Therefore, short-distance wireless technology has an edge over this case. Especially in V2V communication, Dedicated Short Range Communications (DSRC) has been selected as the standard communication protocol. In this paper, we focus on the communication pattern shown in Fig. 1.

We define the information that CAVs can obtain based on this communication pattern as follows:

- Information about the status of the preceding CAV including location, speed, and acceleration;
- Information from the leading CAV that are beyond sensor range or blocked by in-between CAVs;
- Each CAV that follows an MV automatically become the leader, or the subsequent CAV becomes the leader of a new platoon when the number of CAVs reaches the maximum communication scale;

The information transmission mode represented by the green line in Fig. 1 is the CACC system, which enables CAVs to travel with a low headway. The operation of the CACC system is shown in Fig. 2 [26–28]. CACC can be considered an advanced ACC system as it requires additional activation by the DSRC pilot system. In other words, if a CAV follows an MV, the CAV equipped with CACC system degrades to an Automated Vehicle (AV) equipped with ACC system. The blue line represents that the leading CAV is communicating with the following CAVs in the current platoon.

We assume that both CAVs and MVs travel at a constant free-flow velocity v_{opt} until they reach their critical spacing, where the capacity is reached (the word "critical" is dropped hereafter). Considering the effective communication range of the leading CAV, the number of the CAV platoon usually has a certain size limitation S which defines the maximum number of CAVs in a single platoon. In this paper, CAVs with continuous spatial distribution in the same direction are considered to be a flexible platoon. When the size of the platoon reaches S, the subsequent CAVs form another new platoon. This

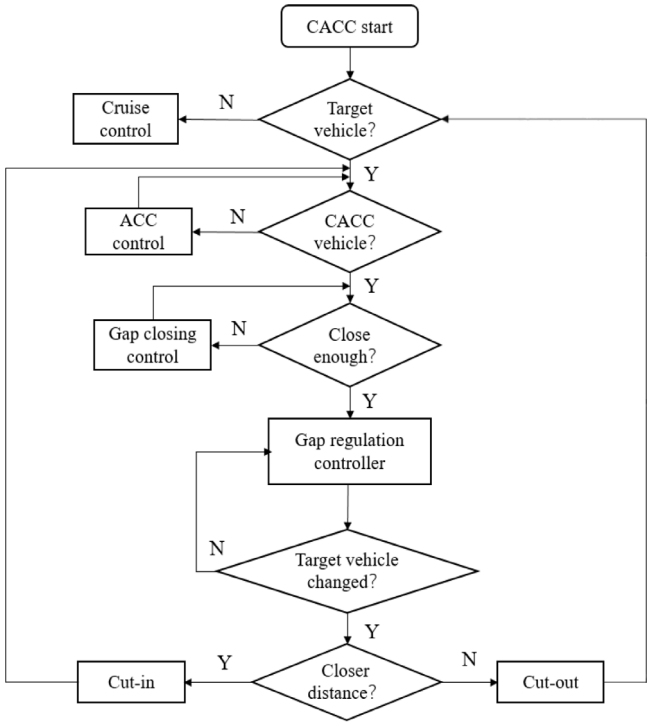

Fig. 2. CACC operation flow chart.

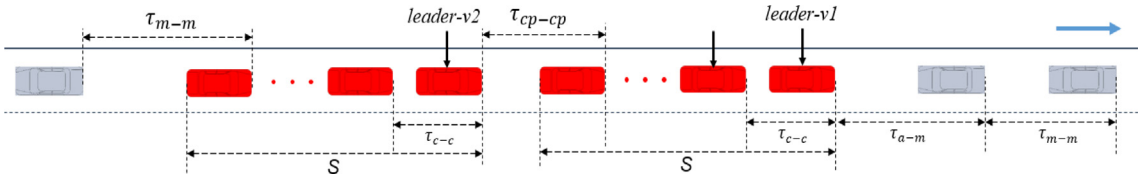

Fig. 3. Illustration of headway in different modes.

means that CAVs on the road can be divided into three categories: a leading CAV following an MV (*leader-v1*), a leading CAV following a CAV (*leader-v2*), and CAVs in the platoon. We assume that a driver is unable to distinguish CAVs from MVs. Therefore, the same car-following model can be applied to MVs whether the leader is a CAV or not. Then, there are four different headway combinations on a one-lane segment as shown in Fig. 3: τ_{m-m}, τ_{a-m}, τ_{c-c} and τ_{cp-cp}, corresponding to MV, *leader-v1*, *leader-v2*, and CAV in the platoon, respectively, and the red vehicles represent CAVs, while the gray ones, represent MVs. They denote the expected headway for an MV following an MV (or CAV), a CAV following an MV, a CAV following a CAV in the same platoon, and a leading CAV following the last CAV of the preceding CAV platoon, respectively.

τ_{m-m} is the maximal headway of the four headways, which is not supported by any on-board sensors or communication equipment. Although some studies suggest that AV with ACC is more sensitive than that of human driving [29], and some points out that the real situation requires a quantitative analysis of headway [30], we believe that AV can operate better based on more accurate sensors and faster decision-making modules in the future. Therefore, τ_{a-m} is smaller than τ_{m-m} in this paper. τ_{c-c} can obtain not only the information of the preceding vehicle but also that of the whole platoon sent by the leader. This information transmission mode can be seen as a more advanced solution than the CACC system so τ_{c-c} is the smallest among all the headways. It is worth noting that τ_{cp-cp} also operates the CACC system, which is higher than τ_{c-c} due to the lack of communication with the preceding platoon.

3. Capacity of mixed traffic

Initially, we defined capacity as the maximum sustainable flow for given proportions of CAVs and MVs in traffic streams (independent of the CAV MPR, p). Also, we defined the penetration rate of *leader-v1*(ACC system operating), *leader-v2*

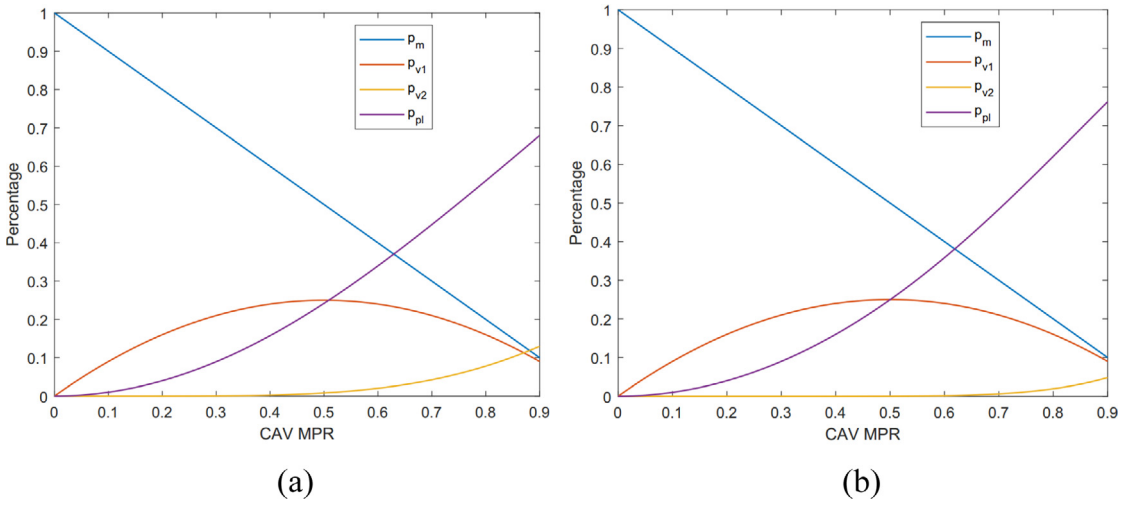

Fig. 4. (a) The percentage of vehicle type changes with the increase of CAV MPR ($S = 5$); (b) The percentage of vehicle type changes with the increase of CAV MPR ($S = 10$).

(CACC system operating), and other CAVs (CACC system operating with CAV platoon gain) in the platoon as p_{v1}, p_{v2} and p_{pl}, respectively. Therefore,

$$p = p_{v1} + p_{v2} + p_{pl}, \tag{1}$$

The penetration rate of MV is

$$p_m = 1 - p, \tag{2}$$

Assuming that all vehicles are mixed randomly and evenly on the road, we can conclude that the penetration rate of *leader-v1* is

$$p_{v1} = p(1 - p), \tag{3}$$

When the number of CAVs in a single platoon reaches limitation S, the next CAV becomes the new leader of another platoon. Then, the average penetration rate of *leader-v2* is

$$p_{v2} = \frac{p^{S+1}(1-p)}{1-p^S}, \tag{4}$$

The penetration rate of CAVs in the platoon is

$$p_{pl} = \frac{p^2 \times \left(1 - p^{S-1}\right)}{1-p^S}, \tag{5}$$

As shown in Fig. 4, the percentage of different vehicle types changes with CAV MPR.

We define τ_{a-m}, τ_{cp-cp}, τ_{c-c} and τ_{m-m} as the headway of *leader-v1*, *leader-v2*, CAV in platoon and MV, respectively. Therefore, the average headway of all vehicles $\widetilde{h}$ on a single-lane is

$$\widetilde{h} = p_{v1} * \tau_{a-m} + p_{v2} * \tau_{cp-cp} + p_{pl} * \tau_{c-c} + p_m * \tau_{m-m}, \tag{6}$$

Additionally, the road capacity for the mixed traffic flow is

$$C_m = \frac{1}{\widetilde{h}} = \frac{1}{p_{v1} * \tau_{a-m} + p_{v2} * \tau_{cp-cp} + p_{pl} * \tau_{c-c} + p_m * \tau_{m-m}}, \tag{7}$$

To simplify this formula, we use a matrix to denote the headway gain. Rewrite Eq. (6) as

$$\tilde{h} = P^T \cdot \boldsymbol{\lambda} \cdot \tau_{m-m}, \tag{8}$$

where $\mathbf{P}$ denotes vehicle penetration rate vector,

$$\mathbf{P} = \begin{bmatrix} p_{v1} \\ p_{v2} \\ p_{pl} \\ p_m \end{bmatrix}, \tag{9}$$

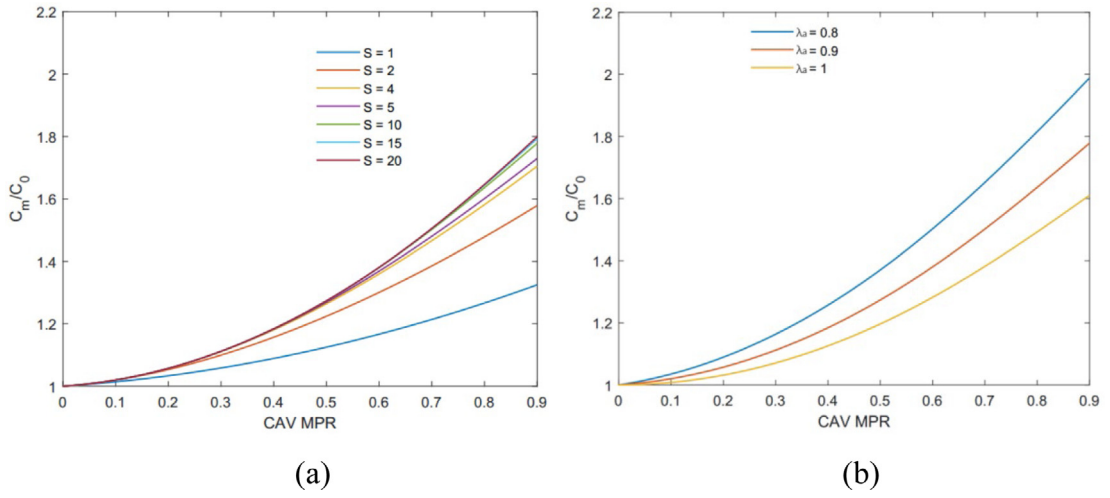

Fig. 5. (a) Capacity gain changes with various p (S from 1 to 20; λ_a=0.9, k_c=0.8 and k_p=0.7) (b) Capacity gain changes with various p ($S = 15$; λ_a from 0.8 to 1.0, k_c=0.8 and k_p=0.7).

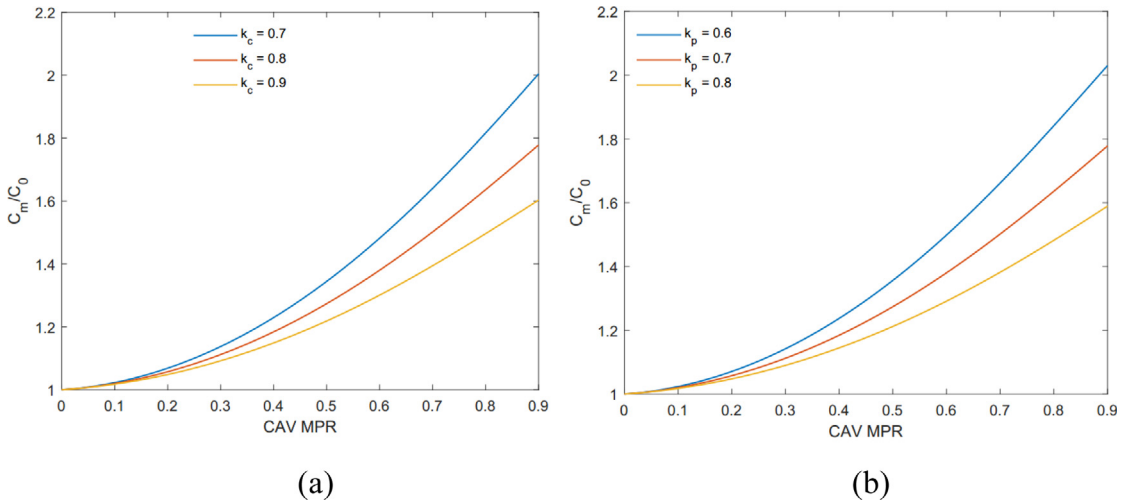

Fig. 6. (a) Capacity gain changes with various p ($S = 15$; λ_a=0.9, k_c from 0.7 to 0.9 and k_p=0.7) (b) Capacity gain changes with various p ($S = 15$; λ_a=0.9, k_c=0.8 and k_p from 0.6 to 0.8).

Similarly, $\boldsymbol{\lambda}$ denotes the headway gain of CAVs to MVs under different states and positions,

$$\boldsymbol{\lambda} = \begin{bmatrix} \lambda_a \\ k_c\lambda_a \\ k_p k_c \lambda_a \\ 1 \end{bmatrix}, \tag{10}$$

where, λ_a, k_c and k_p denote the headway gains of the ACC system over MVs, the CACC over the ACC system, and inter-platoon scenarios, respectively. Assuming that the capacity C_0(no CAV involved) is constant, the capacity gain of C_m over C_0 is

$$\frac{C_m}{C_0} = \frac{1}{\mathbf{P}^T \cdot \boldsymbol{\lambda}}, \tag{11}$$

We performed experiments to compare how different parameters affect road capacity based on Eq. (11). When other parameters are constant, S, λ_a, k_c and k_p are analyzed under different CAV MPR respectively.

As shown in Fig. 5 and Fig. 6, capacity increases significantly with the increase of CAV MPR even under different parameters. Additionally, with the increase of S, or the decrease of λ_a, k_c and k_p, the mixed capacity gain increases

Table 1
Pollutant parameter value [33].

Pollutant	E_0	f_1	f_2	f_3	f_4	f_5	f_6
CO_2	0	3.24e−01	8.59e−02	4.96e−03	−5.86e−02	4.48e−01	2.30e−01
NO_X	0	2.41e−03	−4.11e−04	6.73e−05	−3.07e−03	2.14e−03	1.50e−03
VOC	0	9.22e−05	9.09e−6	−2.29e−07	−2.20e−05	1.69e−05	3.75e−06
PM	0	0.00e+00	3.13e−04	−1.84e−05	0.00e+00	7.50e−04	3.78e−04

correspondingly. It is worth noting that the capacity gain exhibits a nonlinear relationship with CAV MPR. This means that when CAV MPR is low, road capacity will not be improved significantly. However, with a further increase in the number of CAVs, capacity will be rapidly improved. Besides, the effect of the size limitation of the CAV platoons becomes minimal above ten vehicles, while the increase from $S = 5$ to $S = 10$ on capacity is significant. Despite the rapid development of communication range and speed, it is of little help in improving road capacity. On the other hand, enhancing inter-platoon communication can maximize the mixed capacity gain, because it can reduce the headways of inter-platoon CAVs in the most effective manner.

In order to better discuss the influence of each parameter on traffic flow, we solve the partial differential of Eq. (8) with λ:

$$\frac{d\tilde{h}}{d\lambda_a} = p_{v1}\tau_{m-m} + p_{v2}k_c\tau_{m-m} + p_{pl}k_pk_c\tau_{m-m}, \tag{12}$$

As the fundamental parameter that can affect all CAVs, the partial derivative of headway obtained to λ_a has the most significant effect among all headway gain coefficients. Similarly, sensitivity analyses were conducted for other headway gain coefficients.

$$\frac{d\tilde{h}}{dk_c} = p_{v2}\lambda_a\tau_{m-m} + p_{pl}k_p\lambda_a\tau_{m-m}, \tag{13}$$

$$\frac{d\tilde{h}}{dk_p} = p_{pl}k_c\lambda_a\tau_{m-m}, \tag{14}$$

These indicate that the influence of each CAV's headway gain parameter on the mixed headway is linear, and the influence of λ_a is greater than and K_p and k_c.

4. Pollutant emission model

In the relevant research field, several pollutant emission models that reflect their relationship with instant speed and acceleration have been proposed by measuring real urban roads and highways. We developed a pollutant emission model for mixed traffic scenarios based on the speed and acceleration information. We use $E_n(t)$ to describe the pollutant emission for the nth vehicle per unit time and define the parameter according to the relevant literature [31–33]:

$$E_n(t) = \max\left[E_0, f_1 + f_2v_n(t) + f_3v_n(t)^2 + f_4a_n(t) + f_5a_n(t)^2 + f_6v_n(t)a_n(t)\right], \tag{15}$$

where E_0 is the lower pollutant emission limit (g/s) for each vehicle. $f_1 \sim f_6$ are the emission parameters determined by corresponding regression analyses for different types of pollutants. $f_1 \sim f_6$ are the coefficient of constant term, speed, square of speed, acceleration, square of acceleration, product of speed and acceleration, respectively. The following pollution types were modeled: nitrogen oxides (NOx), volatile organic compounds (VOC), carbon dioxide (CO_2), and particulate matter (PM), and all the specified parameter values are listed in Table 1. (Some minor pollutants are neglected)

5. Simulation analyses

It is common to analyze traffic performance and quantify pollutant emissions based on the instant speed and acceleration of vehicles with a microsimulation model. In this section, improved micro car-following models for MVs and CAVs are constructed to simulate the mixed traffic flow and compare the influence of capacity gain and traffic emissions under different headways gains and CAV MPR. The traffic microsimulation model can generate the Spatio-temporal trajectory and measure the speed and acceleration per second throughout the entire moving process of each vehicle. Besides, the models of CAVs are divided into different types according to different states and positions. We then analyze the simulation results and how they change with the increase of CAV MPR.

5.1. Microsimulation model for MVs

In this paper, we use the Full Velocity Difference (FVD) model proposed by Jiang in 2001 [34,35]. This model believes that a vehicle's car-following behavior has two goals. One is to adjust the gap between two vehicles to an appropriate

Table 2
FVD model parameters.

Parameter	α	β	V_1	V_2	C_1	C_2	d
Value	0.41	0.5	14	16	0.13	1.57	5

state, and the other is to reduce the speed difference between the target nth vehicle and the preceding vehicle as much as possible to maintain a stable gap. Besides, the second part of FVD model can reduce the difference between the velocity

$$a_n(t) = \alpha \left[V\left(s_n(t)\right) - v_n(t)\right] + \beta \left(v_{n-1}(t) - v_n(t)\right), \tag{16}$$

$$V\left(s_n(t)\right) = V_1 + V_2 \tanh\left[C_1\left(s_n(t) - d\right) - C_2\right], \tag{17}$$

where α and β are sensitive coefficients, and V_1, V_2, C_1, C_2, d are the optimal velocity parameters. Additionally, $\beta = 0$ when $s_n(t) > 100\,m$. All specific parameters are shown in Table 2.

According to the analysis in Section 2, it is assumed that different CAV modes are only related to the coefficient of different CAV headway gain. To make the car-following model more reliable and convenient to describe the headway, we rewrite Eqs. (13) and (14) as:

$$a_n(t) = \alpha \left[V\left(s_n(t)\right) - v_n(t)\right] + \frac{\beta}{s_n(t)} \left(v_{n-1}(t) - v_n(t)\right), \tag{18}$$

where $s_i\,(t)$ denotes the gap between the target vehicle and the preceding vehicle, thus it can be written as:

$$s_n(t) = x_{n-1}(t) - x_n(t), \tag{19}$$

Therefore, we include headway to describe acceleration with:

$$a_n(t) = \alpha \left[V\left(s_n(t)\right) - v_n(t)\right] + \frac{\beta}{h'_n(t)} - \frac{\beta}{h_n(t)}, \tag{20}$$

where $h_n(t)$ denotes the headway of vehicle n at time t and $h'_n(t)$ denotes the speed of the preceding vehicle divided by the gap between vehicle n and n-1. Put Eq. (10) into Eq. (17), and we can obtain the change of acceleration considering CAVs' headway gain

$$\mathbf{a} = \alpha \left[V\left(s_n(t)\right) - v_n(t)\right] + \frac{\beta}{h'_n(t)} - \frac{\beta}{h_n(t) \cdot \boldsymbol{\lambda}}, \tag{21}$$

In other words, the coefficient of $h_n(t)$ becomes $\beta/\boldsymbol{\lambda}$. Then, we obtain four acceleration type corresponding to different types of vehicles in numerical simulation.

5.2. Microsimulation model for CAVs

We set the parameters of the classical FVD model for MVs, and all models for different CAVs are established under a constant headway. According to Chapter 2, the microsimulation car-following model for CAVs can be divided into three types: *leader-v1* (ACC system operating), *leader-v2* (CACC system operating), and other CAVs (CACC system operating with CAV platoon gain) in the platoon. If the preceding vehicle of a CAV is a CAV, and the space in between is within the V2V communication range, the CACC system activates. Additionally, if the target CAV travels in a CAV platoon, it can further reduce the headway due to the headway gain in CAV platoons. Since we can obtain the mixed traffic capacity model based on the distribution of vehicles' headway, we need a constant headway control system for CAVs. The operational logic of the CACC and ACC controller proposed by PATH Lab satisfies this requirement. Based on the above analyses and field calibration experiments by PATH Lab, we establish a set of CAV updating rules as follows [12,13]:

1. Determine the gap error:

$$e_n(t+1) = x_{n-1}(t+1) - x_n(t+1) - \lambda h_n(t) \cdot v_n(t+1), \tag{22}$$

2. Acceleration:

$$v_n(t+1) = v_n(t) + k_p e_n(t+1) + k_d \dot{e}_n(t+1), \tag{23}$$

3. Safety brake:

$$v_n(t+1) = \max\left\{\min\left(v_n(t+1), v_{\max}\right), 0\right\}, \tag{24}$$

4. Update location:

$$x_n(t+1) = x_n(t) + v_n(t+1)\Delta t, \tag{25}$$

where e_n is the difference between the current gap and the target control gap, and $\lambda h_n(t)$ is the pre-input CAV time headway with gains. We set different headway gains for CAVs in different positions and states as analyzed in Chapter 2. k_p and k_d are the corresponding control parameters, according to the calibration results from the PATH lab. $\dot{e}_n$ is the first derivative of e_n. The specific value of the parameters is shown in Table 3.

Table 3
CAV model parameters.

Parameter	λ for *leader-v1*	λ for *leader-v2*	λ for CAV in platoon	Δt	k_p	k_d
Unit	–	–	–	s	–	–
Value	0.9	0.72	0.5	0.1	0.45	0.25

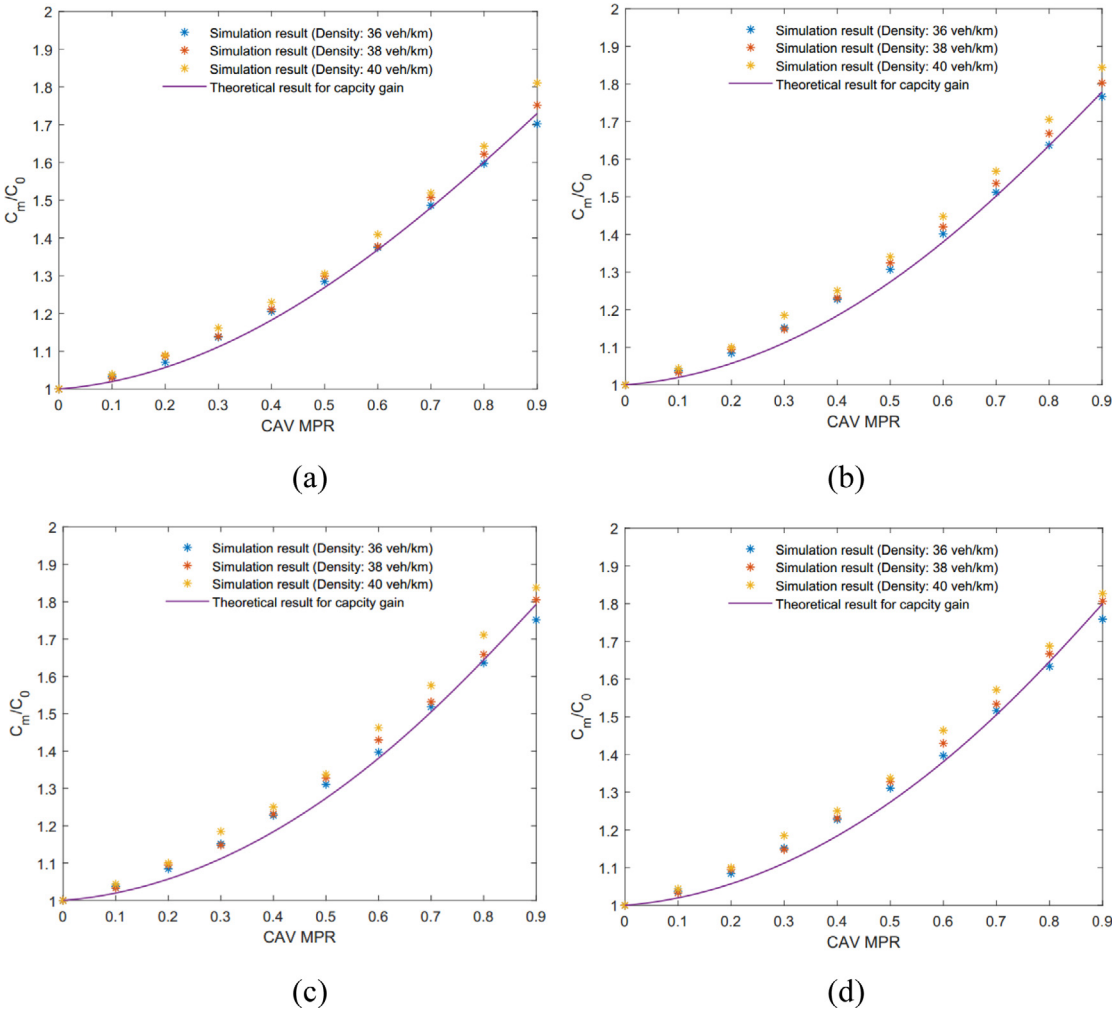

Fig. 7. Capacity gains changes in simulation and theoretical results with various p at a different density. (a) S = 5 (b) S = 10 (c) S = 15 (d) S = 20.

5.3. Simulation results

Towards microsimulation: there are some vehicles on a 5 km single-lane circle road with constant density values (36 veh/km, 38 veh/km, 40 veh/km) and increasing MPR values from 0 to 90%. Each experimental group was operated 100 times under each CAV MPR, and the average result is calculated to minimize random errors. It is worth noting that all car-following models including CAVs and MVs are updated every 0.1 s. Then, the data of CAV model is recorded at each update, but that of MV model is recorded every 10 time steps.

As shown in Fig. 7, the theoretical results in Chapter.2 are highly consistent with the simulation results. Relatively speaking, the simulation results are more similar under a high density, which means CAVs can improve the optimal range of traffic density. Additionally, the capacity gains are similar in $S = 10$, $S = 15$, and $S = 20$, but they all have a significant increase over the capacity gains in $S = 5$.

RMSE is a non-robust prediction evaluation index highly sensitive to errors, while MAPE considers the error proportion and has remarkable robustness. They are applied in this paper as a reference to reflect the difference between the theoretical and simulation results (see Table 4).

Thus, we can believe that these two results are highly correlated.

Table 4
Comparison between the theoretical and simulation results.

INDEX	S = 5			S = 10			S = 15			S = 20		
	36 veh/km	38 veh/km	40 veh/km	36 veh/km	38 veh/km	40 veh/km	36 veh/km	38 veh/km	40 veh/km	36 veh/km	38 veh/km	40 veh/km
RMSE	0.199	0.180	0.173	0.198	0.177	0.176	0.177	0.165	0.150	0.161	0.140	0.143
MAPE	16.95	15.37	14.62	16.94	15.09	14.69	14.70	13.51	12.80	13.10	11.91	12.11

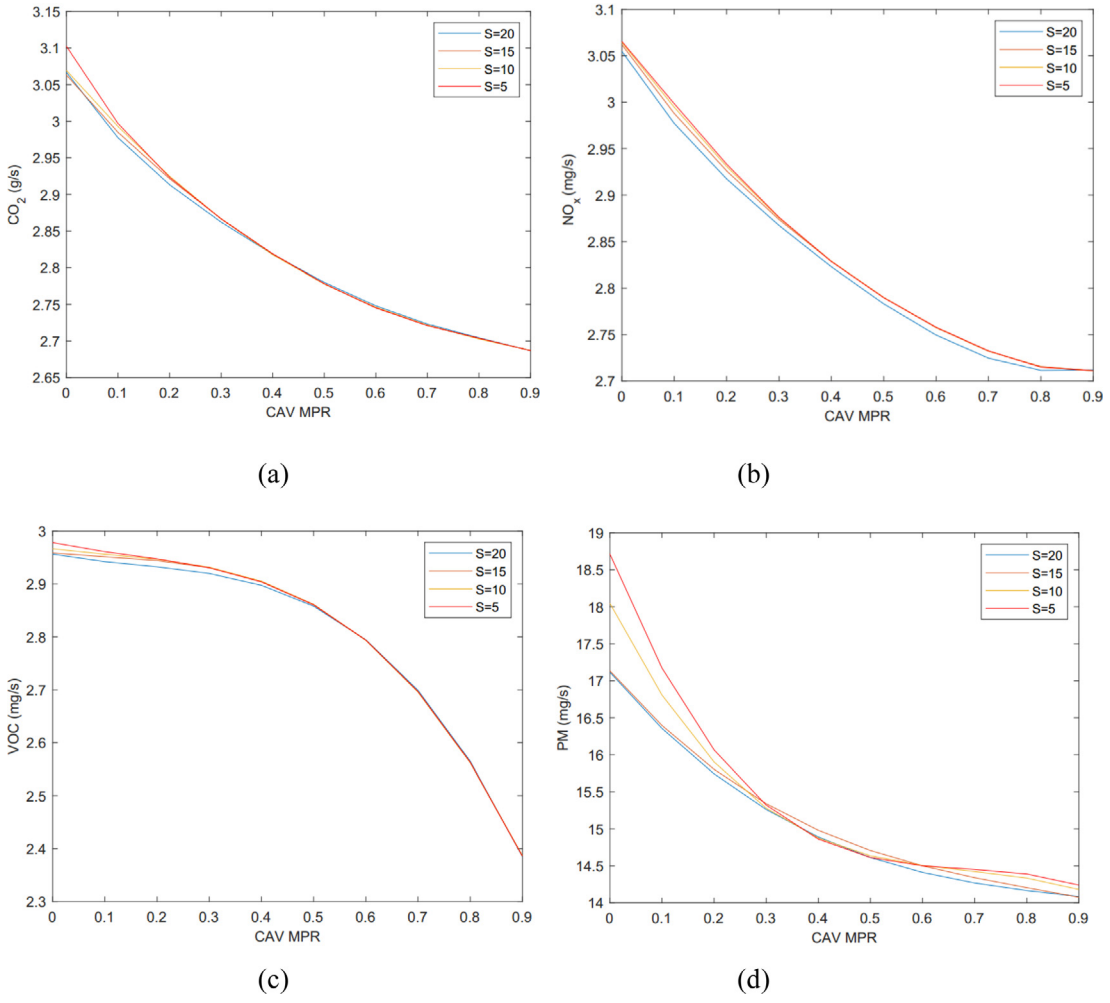

Fig. 8. (a) Emission of CO_2 changes with different CAV MPR; (b) Emission of NO_x changes with different CAV MPR (c) Emission of VOC changes with different CAV MPR (a) Emission of PM changes with different CAV MPR (*S* from 5 to 20).

It is common to analyze traffic performance and quantify pollutant emissions based on the instant speed and acceleration of vehicles with a microsimulation model. The traffic microsimulation model can generate the Spatio-temporal trajectory and measure the speed and acceleration per second throughout the entire moving process of each vehicle.

Based on this formula, we can calculate the emissions per time with speed and acceleration, which can be obtained in the microsimulation.

The CO_2, NOx, VOC, and PM emissions in this simulation are shown in Fig. 8 as the increase of CAV MPR at different *S* ranging from 5 to 20.

As shown in Fig. 8, the result of numerical simulation indicates that there is a significant decrease in pollutant emission with the increase of CAV MPR. However, with different platoon size limitations, these descending trends are not the same.

In terms of the overall trend of emissions change, CO_2, PM and NOx exhibit similar patterns which all decrease gradually with CAV MPR, but the rate of reduction decreases gradually. The emission of VOC is on the contrary, whose rate of

reduction increases gradually. By comparing the parameters in Eq. (15) with the values in Table 1, it is indicated that VOC emission model has a higher weight in the coefficient of acceleration, that is f_4, compared with the other three pollutants. The reason for that is that both the traffic flow and average velocity of the mixed vehicles can be calculated according to Eq. (11) with a given CAV MPR and density. Therefore, what further affects pollutant emissions is the change in acceleration. Obviously, the increase of CAV MPR is helpful to improve the stability of the CAV platoon, that is, to reduce unnecessary acceleration and deceleration behavior, thus reducing pollutant emissions. According to this reasoning, CO_2, PM and NOx all have higher weight on f_1, f_2 and f_6 which are the coefficients of velocity. For VOC, the highest weight is the coefficient of acceleration, and this means that as the CAV MPR increases, the average speed of the team exhibits a marginal diminishing increase, but the acceleration and deceleration can still be reduced. Towards platoon size limitations S, CO_2, VOC and NOx are similar, their changes under different S are basically similar (only a slightly decrease with S), that is, increasing the size of the platoon does not significantly change pollutant emissions, while the amount of PM decreases significantly when S is less than 15.

6. Conclusion

In this paper, we developed a road capacity gain formula for mixed traffic flow which varies with CAV MPR and several parameters. The FVD model and CAV model were used to simulate the MV–CAV mixed flow. Based on the simulation, the impacts of CAVs on the capacity and pollutant emissions were studied. The main conclusions are as follows.

CAVs contribute to a significant increase in road capacity as CAV MPR increases. Some major parameters, like headway gains and platoon size, have significant impacts on capacity gain. However, the platoon size has little effect on road capacity when it is over 10. This means that the optimal size of CAV platoons is around 10 when considering only the capacity gain.

For pollutant emissions, CAVs can help reduce pollution significantly. Among them, the marginal effect of CO2, PM and NOx decreases with CAV MPR, while that of VOC increases. For CAV platoon size limitation, there is a little benefit of enlarging platoon size when the CAV platoon size is over 5 for CO2, VOC and NOx, while there is a significant benefit for PM. However, when the platoon size is over 15, the benefits of enlarging platoon size are insignificant. Therefore, a platoon size between 5 and 10 may be appropriate when taking both the road capacity and pollutant emissions into account.

The rapid development of CAV technologies has attracted the attention of many researchers. To ensure the stable and environmental-friendly operation of CAVs, further experiments are needed. In this paper, we developed a capacity gain formula for CAV platoons, but it has not been verified in field tests. The impacts of V2V communication topologies on the mixed traffic flow need field tests, which will be conducted by us in the future.

CRediT authorship contribution statement

Ke Ma: Conceptualization, Model, Writing – original draft. **Hao Wang:** Supervision, Editing. **Tiancheng Ruan:** Code.

Declaration of competing interest

The authors declare that they have no known competing financial interests or personal relationships that could have appeared to influence the work reported in this paper.

Acknowledgments

This research was sponsored by the National Key Research and Development Program of China (No. 2019YFB1600200) and National Science Foundation of China (No. 51878161 and No. 52072067.)

References

[1] Zachary Vander Laan, K.F. Sadabadi, Operational performance of a congested corridor with lanes dedicated to autonomous vehicle traffic, Int. J. Transp. Sci. Technol. 6 (1) (2017) 42–52.
[2] Liang Zheng, P.J. Jin, H. Huang, An anisotropic continuum model considering bi-directional information impact, Transp. Res. B 75 (2015) 36–57, b.may.
[3] Wang, Meng, Infrastructure assisted adaptive driving to stabilise heterogeneous vehicle strings, Transp. Res. C 91 (2018) 276–295.
[4] Ye, et al., Evaluation of the impacts of cooperative adaptive cruise control on reducing rear-end collision risks on freeways, Accid. Anal. Prev. (2017).
[5] Wang Hao, et al., Stability of CACC-manual heterogeneous vehicular flow with partial CACC performance degrading, Transp. B Transp. Dyn. (2018) 1–26.
[6] Jun Lee, J.H. Kim, Phantom traffic: Platoon formed at low traffic density, J. Transp. Eng. 145 (2) (2019) 04018082.1-04018082.7.
[7] Zhu Wen-Xing, Z. Li-Dong, A new car-following model for autonomous vehicles flow with mean expected velocity field, Physica A 492 (2018) 2154–2165.
[8] YaoMing Yuan, Traffic flow characteristics in a mixed traffic system consisting of ACC vehicles and manual vehicles: A hybrid modeling approach, in: World Congress on Intelligent Transport Systems & Its Americas Meeting 2008.
[9] Sun, et al., An extended car-following model under V2V communication environment and its delayed-feedback control, Physica A (2018).

[10] Raphael E. Stern, et al., Dissipation of stop-and-go waves via control of autonomous vehicles: Field experiments, Transp. Res. C 89 (2018) 205–221.
[11] Noah J. Goodall, B. Park, B.L. Smith, Microscopic estimation of arterial vehicle positions in a low-penetration-rate connected vehicle environment, J. Transp. Eng. 140 (10) (2014) 04014047.1-04014047.9.
[12] Vicente Milanes, S.E. Shladover, Modeling cooperative and autonomous adaptive cruise control dynamic responses using experimental data, Transp. Res. 48 (2014) 285–300, c.nov.
[13] K. Ma, H. Wang, Influence of exclusive lanes for connected and autonomous vehicles on freeway traffic flow, IEEE Access (2019).
[14] Chaojie Wang, et al., Cooperative adaptive cruise control for connected autonomous vehicles by factoring communication-related constraints, Transp. Res. Procedia 38 (2019) 242–262.
[15] Qin Yanyan, W. Hao, R. Bin, Stability analysis of connected and automated vehicles to reduce fuel consumption and emissions, J. Transp. Eng. A Syst. 144 (11) (2018) 04018068-.
[16] K. Ma, H. Wang, How connected and automated vehicle–exclusive lanes affect on-ramp junctions, J. Transp. Eng. A Syst. (2021).
[17] D. Chen, S. Ahn, M. Chitturi, et al., Towards vehicle automation: Roadway capacity formulation for traffic mixed with regular and automated vehicles, Transp. Res. 100 (2017) 196–221, jun.
[18] X. Fu, W.H.K. Lam, Modelling joint activity-travel pattern scheduling problem in multi-modal transit networks, Transportation (2018).
[19] Steven Shladover, D. Su, X.Y. Lu, Impacts of cooperative adaptive cruise control on freeway traffic flow, Transp. Res. Record J. Transp. Res. Board 2324 (2012) 63–70.
[20] F.Y. Liu, H. Wang, C. Dong, Q. Chen, A car-following data collecting method based on binocular stereo vision, IEEE Access 8 (2020) 25350–25363, http://dx.doi.org/10.1109/ACCESS.2020.2965833.
[21] D. Mcdougall, R.O. Moore, Optimal strategies for the control of autonomous vehicles in data assimilation, Physica D 351–352 (2017) 42–52.
[22] Changyin Dong, et al., Economic comparison between vehicle-to-vehicle (V2V) and vehicle-to-infrastructure (V2I) at freeway on-ramps based on microscopic simulations, IET Intell. Transp. Syst. 13 (11) (2020) 1726–1735.
[23] D. Li, C. jie Jin, M. Yang, A. Chen, Incorporating multi-level taste heterogeneity in route choice modeling: From disaggregated behavior analysis to aggregated network loading, Travel Behav. Soc. (2020).
[24] Yanyan Qin, H. Wang, B. Ran, Ran impact of connected and automated vehicles on passenger comfort of traffic flow with vehicle-to-vehicle communications, Ksce J. Civ. Eng. (2018).
[25] Jin I. Ge, et al., Experimental validation of connected automated vehicle design among human-driven vehicles, Transp. Res. 91 (2018) 335–352, JUN.
[26] Z. Yao, T. Xu, Y. Jiang, R. Hu, Linear stability analysis of heterogeneous traffic flow considering degradations of connected automated vehicles and reaction time, Physica A (2021).
[27] Z. Yao, R. Hu, Y. Wang, Y. Jiang, B. Ran, Y. Chen, Stability analysis and the fundamental diagram for mixed connected automated and human-driven vehicles, Physica A (2019).
[28] X. Chang, H. Li, J. Rong, X. Zhao, A. Li, Analysis on traffic stability and capacity for mixed traffic flow with platoons of intelligent connected vehicles, Physica A (2020).
[29] J. Lioris, R. Pedarsani, F.Y. Tascikaraoglu, P. Varaiya, Platoons of connected vehicles can double throughput in urban roads, Transp. Res. C (2017).
[30] A. Ghiasi, O. Hussain, Z. (Sean) Qian, X. Li, 30 analysis and lane management model for connected automated vehicles: A Markov chain method, Transp. Res. B (2017).
[31] C. Wang, Z. Sun, Z. Ye, On-road bus emission comparison for diverse locations and fuel types in real-world operation conditions, Sustainability (2020).
[32] W.X. Zhu, Analysis of CO_2 emission in traffic flow and numerical tests, Physica A (2013).
[33] X. Wang, Y. Xue, B. ling Cen, P. Zhang, H. di He, Study on pollutant emissions of mixed traffic flow in cellular automaton, Physica A (2020).
[34] Rui Jiang, Q.S. Wu, Cellular automata models for synchronized traffic flow, J. Phys. A General Phys. 36 (2) (2002) 381.
[35] Rui Jiang, Q.S. Wu, First order phase transition from free flow to synchronized flow in a cellular automata model, Eur. Phys. J. B 46 (4) (2005) 581–584.